

Modal analysis of butt-welded aluminum alloy beams with different welding root widths

Farklı kaynak kökü genişliklerine sahip alın kaynaklı alüminyum alaşımı kırışının modal analizi

Muhammet Raci AYDIN* 

Iğdır University, Faculty of Engineering, Department of Mechanical Engineering, 76000, Iğdır

• Received: 21.04.2025

• Accepted: 16.07.2025

Abstract

In this study, the effect of different welding root widths on the vibrational behavior of butt-welded aluminum alloy structures was investigated using numerical methods. Specimens with dimensions of $250 \text{ mm} \times 25 \text{ mm} \times 5 \text{ mm}$ and free-free boundary conditions were modeled in ANSYS Workbench® finite element software, including a weld-free reference specimen and specimens with V-shaped joints at a 60° angle having welding root widths of 0, 1, 2, 3, and 4 mm. Natural frequencies and mode shapes were determined and the first three natural frequencies of the unwelded specimen were calculated based on the Euler-Bernoulli beam theory for comparison. A good agreement was observed between the two methods. The results indicated that geometric variations in the welding region affect the mass-volume values and structural stiffness. In specimens with 0 mm root width, frequency values decreased, while an increasing trend in the first and third natural frequencies was observed for root widths between 1-4 mm. A maximum change of 1.34% was found between the 4 mm welding root specimen and the reference. The second natural frequency remained unchanged, as the welded region corresponded to the node location of the second mode shape. This study is novel in that it investigates the effect of different root widths on vibration behavior. In the future, theoretical, numerical, and experimental studies will be conducted using different material and welding parameters.

Keywords: Al alloy beam, Butt weld, Euler-Bernoulli, Modal analysis, Mode shapes, Natural frequency

Öz

Bu çalışmada, farklı kaynak kök genişliklerinin alın kaynaklı alüminyum alaşımı yapılarının titreşim davranışlarına etkisi sayısal yöntemlerle incelenmiştir. $250 \text{ mm} \times 25 \text{ mm} \times 5 \text{ mm}$ boyutlarında, serbest-serbest sınır şartlarına sahip referans numune ile 0, 1, 2, 3 ve 4 mm kaynak kök genişliğine sahip V-şeklinde 60° açılı birleşimlere sahip numuneler ANSYS Workbench® sonlu elemanlar yazılımında modellenmiştir. Doğal frekans ve mod şekilleri belirlenmiş, kaynaksız numune için Euler-Bernoulli teorisine göre hesaplanan ilk üç doğal frekans değerileyile karşılaştırılmıştır. İki yöntem arasında iyi bir uyum görülmüştür. Sonuçlar, kaynak bölgesindeki geometrik değişimin kütle-hacim değerleri ve yapısal rıjilik üzerinde etkili olduğunu göstermiştir. 0 mm kök genişliğine sahip numunelerde frekanslar düşerken, 1-4 mm arasında özellikle birinci ve üçüncü doğal frekanslarda artış gözlenmiştir. 4 mm kök genişliğine sahip numune ile referans numunesi arasında maksimum %1,34'lük bir fark tespit edilmiştir. Kaynaklı bölgenin node bölgesine denk geldiği ikinci mode şeklinde ikinci doğal frekans değeri değişmemiştir. Bu çalışmanın yeniliği, farklı kaynak kök genişliklerinin titreşim davranışının etkisinin araştırılmasıdır. Gelecekte farklı malzeme ve kaynak parametreleri kullanılarak teorik, sayısal ve deneyel çalışmalar yürütülecektir.

Anahtar kelimeler: Al合金 kırış, Alın kaynağı, Euler-Bernoulli, Modal analiz, Mod şekilleri, Doğal frekans

1. Introduction

Aluminium alloys have attracted significant interest across various industries thanks to their high strength-to-weight ratio, excellent formability and corrosion resistance. Butt welding is a process used to join two metal pieces end-to-end, offering high strength and low weight advantages. This method is utilized in various industrial applications, including aerospace, energy, automotive, construction, shipbuilding, and pipelines. This method has disadvantages such as precise alignment and the need for more filler material compared to

*Muhammet Raci AYDIN; mraici.aydin@igdir.edu.tr

some other welding methods, but its advantages such as aesthetic appearance, good penetration, strength and liquid/gas tightness make it popular for joining structural materials of certain thicknesses (Mathers, 2002; Etinosa & Achebo, 2017). Aluminum is preferred to other metals because of its advantages such as high strength, low density, electrical conductivity, resistance to oxidation, water and salt corrosion (Imran & Verma, 2021). The filler metal used in welding melts and solidifies with the base metal to form the weld metal. Manufacturers try to ensure that the filler metal is as similar as possible to the mechanical properties of the rolled base metal. The maintenance of properties, such as strength, ductility and notch impact resistance, is of particular significance. For many purposes, the strength of the filler material in butt welding is considered the same as the base metal and may not be considered separately for calculating the static strength of the structure (Hicks, 2000). In the study by Hatifi et al. (2014), the effect of butt welding of different metal plates of different thicknesses (stainless steel and aluminum alloy) on the modal properties was compared by experimental and numerical analysis. It was observed that the experimental and numerical results were in good agreement. ANSYS® software results were compared with experimental results for vibration-based damage detection in welded structures and good agreement was observed between both methods. Such software can significantly reduce the cost and time of repeated experiments (Rao & Ratnam, 2012).

Welding is the most widely used method of permanent joining. Butt-welding is used for joining parallel and non-overlapping parts. Welding damage due to vibrations can be minimized by considering the modal vibration characteristics of the material. Etinosa & Achebo (2017) analyzed the natural frequencies and mode shapes of butt-welding joints with five different shapes. There are also studies on welded lap joints other than butt welded joints. Bhusnar & Sarawade (2016) performed modal analysis to find the natural frequencies and mode shapes of Al plates with welded lap joint. The results were compared with different joint types. Additionally, thermal stresses and residual stresses in the weld zone during welding can cause a decrease in the natural frequency of the structure. Welding is a comprehensive and multi-physical process in which heat transfer, fluid motion and stress arising all happen simultaneously (Das et al., 2020). Repetitive stresses can lead to fatigue after a period. This can lead to vibration-induced damage (premature or sudden). In addition, the temperature increase in the weld zone can change the mechanical properties of the base metal and reduce its strength. Unwelded base metal under vibration is more durable than welded joints. The location, shape, and width of the welding joint substantially affect dynamic performance, structural strength, and reliability. There are also experimental and numerical studies that consider the weld residual stress in butt-welded metal joints in terms of various properties (Pavani et al., 2015; Macanhan et al., 2019; Arruda et al., 2023). Apart from these, studies have also been carried out using ANSYS® software to simulate bending and torsional loads for different cross-sectional areas and compare the results with analytical solutions. The weld location, shape, and root width have a significant influence on the dynamic performance, structural strength, and reliability (Thirugnanam et al., 2014). In addition to the above studies, there are various studies in the literature on the modeling and analysis of the dynamic behavior of braced structures. Gharehbaghi et al. (2023) investigated the residual stresses formed in aluminum sheet metal after the welding process both experimentally and numerically using ABAQUS software; in the numerical modeling, they defined the welding region and the base material as a single material. AbuShanab & Moustafa (2018) joined AA1060 aluminum specimens with different defect geometries using the Friction Stir Welding (FSW) method, conducted both experimental vibration tests and analysis using ANSYS® software, and demonstrated that damping capacity is a more sensitive indicator than natural frequency in determining welding defects.

In Khurshid's (2017) doctoral thesis, static and fatigue analyses were performed on steel welded structures; although the weld and HAZ regions were modeled separately, the models were simplified by using the same elasticity modulus for all regions. Similarly, Resan & Jasim (2022) investigated the bending behavior of aluminum beams with different cross-sections both experimentally and numerically and defined a single elastic model for the entire structure. Chandravanshi & Mukhopadhyay (2013) modeled a two-story structure with the same material properties and performed modal analysis in the ANSYS Workbench® 14 software, evaluating frequency and damping parameters. These studies generally addressed the welding region without modeling it as a separate material, proceeding under the assumption of material homogeneity. In this context, the presented study makes an important contribution to the existing literature by detailing the effect of geometric variations in the welding region on vibration behavior.

In this study, the vibration behavior of aluminum beams was investigated using numerical methods, taking into account the effect of different welding root widths. The dynamic properties of welding structures are of great importance in terms of structural stability and strength. However, there are very few studies in the

relevant literature that directly address the effect of different welding root widths on natural frequency variation. A numerical model validated using Euler-Bernoulli theory and the finite element method was adapted for different root widths and a comparative analysis was performed. This study contributes to the relevant literature by both aiding in the optimization of welding parameters in engineering applications and introducing a new evaluation perspective for vibration-based structural analyses.

2. Material and method

2.1. Material

The material properties of the Al alloy such as Young's modulus, density and Poisson's ratio were taken from the material library of the ANSYS19 Workbench® analysis program (Table 1). In ANSYS Workbench®, a material with "Isotropic Elasticity" properties assumes that the material's elastic behavior is the same in all directions. This situation generally applies to homogeneous and uniform metallic materials. In welded metallic structures, the weld metal, heat-affected zone (HAZ), and base metal typically exhibit different mechanical properties. In thermo-mechanical analyses, particularly those considering fatigue or crack growth, these regions must be modeled with different properties. However, especially in "initial approaches" or in modal analyses (natural frequency, mode shape) performed using the finite element method (FEA) where only geometric effects (mass, volume) are considered, it is acceptable to assume that these regions have the same material properties (Chandrvanshi & Mukhopadhyay, 2013; Bhusnar & Sarawade, 2016; Etin-osa & Achebo, 2017; Khurshid, 2017; AbuShanab & Moustafa, 2018; Resan & Jasim, 2022; Gharehbaghi et al., 2023). This approach simplifies modeling and saves time in initial approaches analyses. In this study, the mass and volume parameters affecting vibration characteristics are very small values compared to the main material in the welded region. Considering the findings obtained, more detailed studies will be conducted in experimental analyses. For this reason, the welded material and the main material are defined as having the same properties using a similar approach with the relevant literature.

Table 1. Material properties of the Al alloy used in the numerical analysis (ANSYS®, 2019)

Aluminum alloy	Value
Density (kg/m ³)	2770
Young's modulus (MPa)	71000
Bulk modulus (MPa)	69608
Shear modulus (MPa)	26692
Poisson's ratio	0.33

2.2. Method

The beams to be numerically modally analysed were modelled using the SolidWorks® 2020 program. The joint surface of the weld zone was modelled as a "V" shape with an angle of 60° and a total beam length of 250 mm. In addition, widths of the weld sub-base were created at 1 mm intervals from 0 mm to 4 mm. The weld area and geometry of the beams were designed to be similar to practical applications (Figure 1).

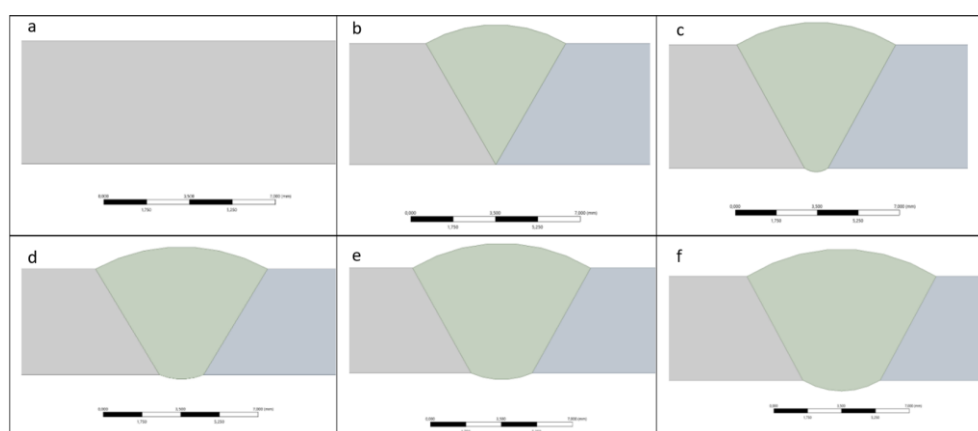


Figure 1. Cross-sections of the middle regions of the beams analyzed by FEM; a) the reference specimen and b) 0 mm, c) 1 mm, d) 2 mm, e) 3 mm, f) 4 mm, specimens with weld root base width.

2.2.1. Theoretical analysis (Euler-Bernoulli thin beam theory)

The vibration analysis of the reference specimens analyzed in this study used the Euler-Bernoulli theory of beam bending, also known as the Euler-Bernoulli or thin beam theory, instead of the thick beam theory or Timoshenko beam theory, which takes into account the effects of rotational inertia and shear deformation because the cross-sectional dimensions are small compared to the length of the beam (Rao, 2006). The material properties used in the numerical analysis were used to calculate the first three in-plane mode shapes and natural frequency (ω_n) values for the reference specimen (250 mm \times 25 mm \times 5 mm) for the free-free boundary condition. In Figure 2, the function $W(x)$ is known as the normal mode or the characteristic function of the beam. β_nl is the frequency parameter and its value varies according to the boundary conditions and mode shapes. The values of β_nl for the first three modes are $\beta_1l=4.730$, $\beta_2l=7.853$, $\beta_3l=10.996$ respectively. ω_n is called the natural frequency of vibration (equations 1-2). Where E is Young's modulus, and I is the moment of inertia of the beam cross-section about the y-axis. ρ is the bulk density of the material, A is the cross-sectional area of the beam, l is the length of the beam (Rao, 2019).

$$\omega_n = (\beta_nl)^2 \sqrt{\frac{EI}{\rho Al^4}} \quad (1)$$

$$\beta_nl \approx (2n + 1) \frac{\pi}{2}, \quad (n = 1, 2, 3, \dots) \quad (2)$$

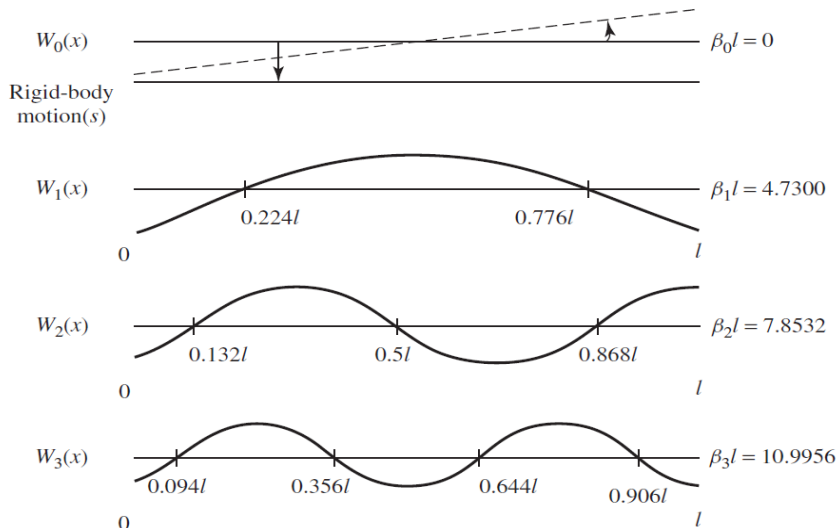


Figure 2. Natural frequencies and mode shapes of a beam with free ends (Rao, 2019).

2.2.2. Numerical analysis (ANSYS Workbench®)

Numerical modal analyses were performed on all specimens shown in Table 2 using the ANSYS Workbench® package program, which generates finite element method (FEM) solutions. The effect of different welding root widths and weld geometries on the dynamic properties of the beam, with respect to the free boundary condition, was investigated. The first three in-plane mode shapes and natural frequency variations are evaluated considering the effect of weld area, stiffness and mass.

Table 2. Specimen dimensions used in numerical analysis

Dimensions	Reference specimens (mm)	Welding root widths				
		0 mm	1 mm	2 mm	3 mm	4 mm
Length (mm)	250	250	250	250	250	250
Width (mm)	25	25	25	25	25	25
Thickness (mm)	5.00	5.77	6.06	6.26	6.48	6.83

The last row of Table 2 shows the top-level thickness of the reference specimen and the welded beams. From Table 2, it can be seen that as the bottom base spacing increases, the volume and weight values that affect the modal properties of the welded beam increase. The general structure of the analysed material is rectangular prism-shaped, therefore regular polygonal structural elements, referred to as “homogeneous structural solid geometry” as presented in Figure 3.a, were used in the mesh structure. In the numerical analysis of the beams, Solid186 was used for the beam in general and Targe170 and Conta174 mesh structural elements were used for the welded surfaces and beam-weld connection areas. Solid186 is a 3D mesh element with 20 nodes and each node has freedom in x, y, z directions. Conta174 mesh elements were used to model the surface-to-surface and/or node-to-surface contact areas. Targe170 mesh structure was used in the node-surface or line-surface contact region (Figure 3).

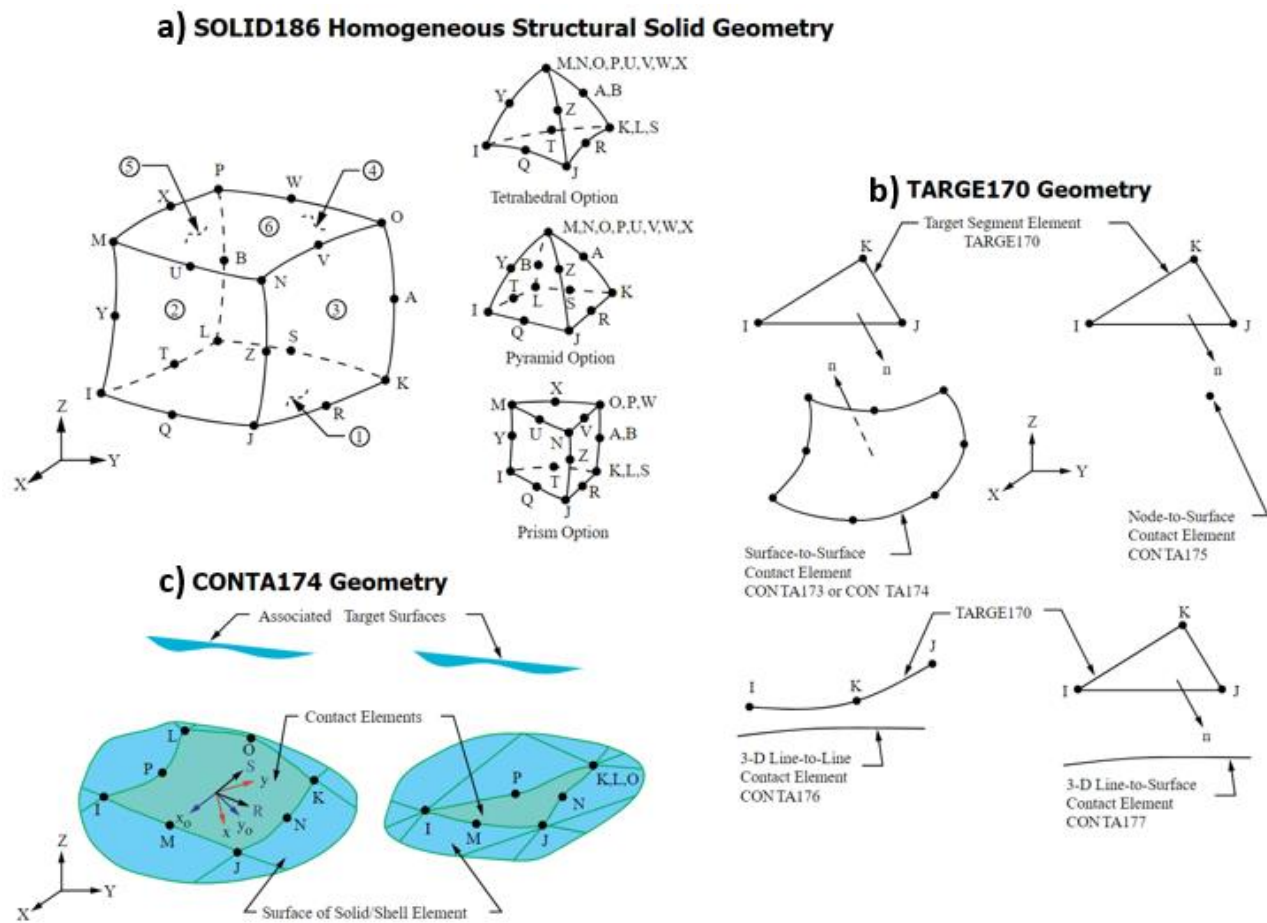


Figure 3. Structural mesh elements used in numerical analysis, a) Solid186; b) Target170, c) Conta174 (ANSYS®, 2025).

3. Results and discussion

The first three natural frequencies of the reference specimen calculated theoretically (Euler-Bernoulli) and the frequency values determined by numerical analysis (ANSYS Workbench®) are very close to each other. The calculated % error rates for the first three natural frequencies are 0.09, 0.22 and 0.43, respectively (Table 3). The error (%) values presented in Table 3 were calculated according to equation 3.

$$\text{Error (\%)} = \frac{(\text{Euler-Bernoulli}) - (\text{ANSYS})}{(\text{Euler-Bernoulli})} \cdot 100 \quad (3)$$

The lowest volume and mass values belong to the reference sample without welding. An increase in volume and mass values was observed with an increase in the root distance of the lower weld. Depending on the volume increase, the number of nodes varies between 9065 and 9326, and the number of elements varies between 1512 and 1530 (Table 4).

Table 3. Theoretical and numerical analysis results (first three natural frequencies) and % error for reference specimens

Natural frequencies (Hz)	Euler-Bernoulli	ANSYS®	Error (%)
ω_1	416.32	415.95	0.09
ω_2	1147.57	1145.10	0.22
ω_3	2249.98	2240.30	0.43

The element size was taken as 3 mm. While the average element quality in the mesh structure of the reference specimen without welding is 0.98492, it is 0.94138 in the specimen having the 4 mm weld root distance where the volume variation is the highest.

The theoretically calculated frequency values and the frequency values determined by numerical analysis are very close to each other. The volume and mass changes of the models and the number of nodes and elements obtained as a result of the meshing process are presented in Table 4.

Table 4. Volume and mass values of the numerical models and the number of nodes and elements obtained as a result of the meshing

Dimensions	Reference specimen	Welding root widths				
		0 mm	1 mm	2 mm	3 mm	4 mm
Volume (mm ³)	31250	31325	31356	31394	31440	31501
Mass (kg)	0.0865	0.0868	0.0869	0.0870	0.0871	0.0873
Number of nodes	9065	9511	9433	9433	9540	9326
Number of elements	1512	1566	1548	1548	1566	1530

Figure 4.a shows the isometric mesh image of the reference specimen used in the numerical analysis. Figure 4.b-c and d show the first, second and third mode shapes respectively. Figure 4.a illustrates the isometric shape of the reference specimen' with a regular rectangular mesh structure. Figure 4.b presents the deformation shape formed in the first mode according to the free-free boundary condition. As can be seen from the figure, two non-vibrating node regions have formed in the first mode shape. Figure 4.c shows three non-vibrating node regions formed according to the second mode shape. Figure 4.d displays four non-vibrating node regions formed according to the third mode shape. In all mode shapes, the maximum deformation is observed at the end points colored red.

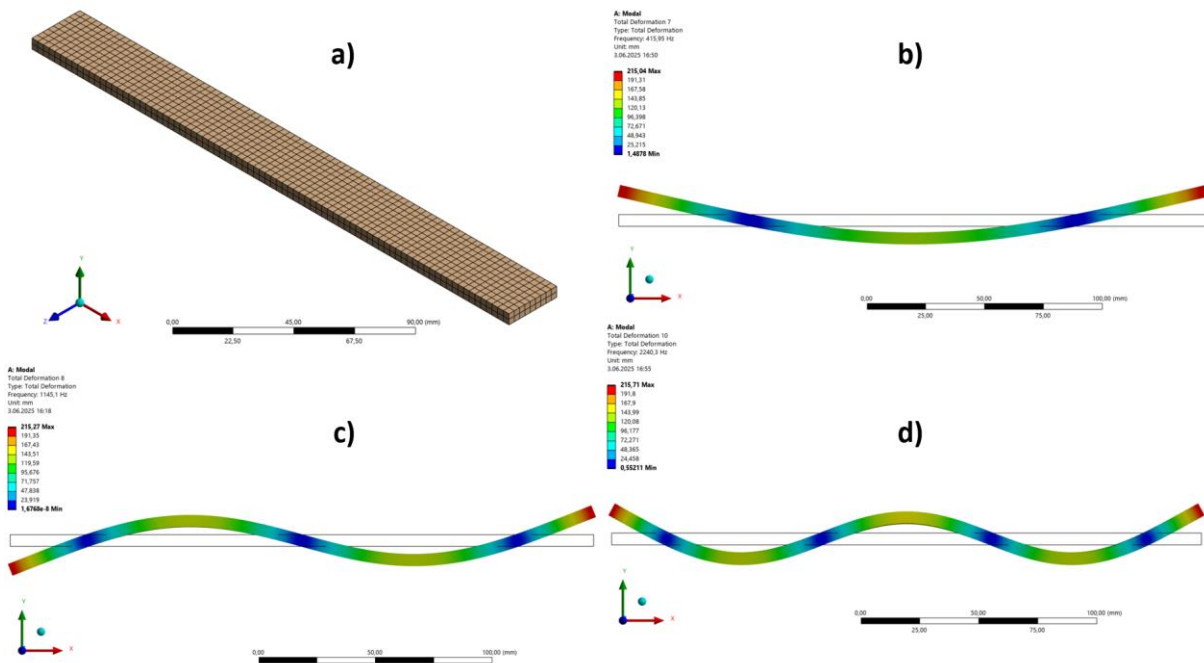
**Figure 4.** a) Isometric shape of the reference specimen, b) first mode shape, c) second mode shape, d) third mode shape

Figure 5 shows the isometric shape of the welded specimens. Figure 5.a shows the mesh structure of the welded beam; b, c and d show the first, second and third isometric mode shapes respectively. Figure 5 illustrates the mesh structure and isometric mode shapes of the welded specimens with a 4 mm weld root width. Comparison with Figure 4 shows that the butt welding in the middle region does not cause any change in the general mode shapes of the specimens. In Figure 5.c, the node region formed in the exact middle region according to the second mode shape coincides with the welding region. This situation explains why the second natural frequencies remain unchanged. In other words, changes in mass and volume on the node region do not alter the relevant frequency values up to a certain level.

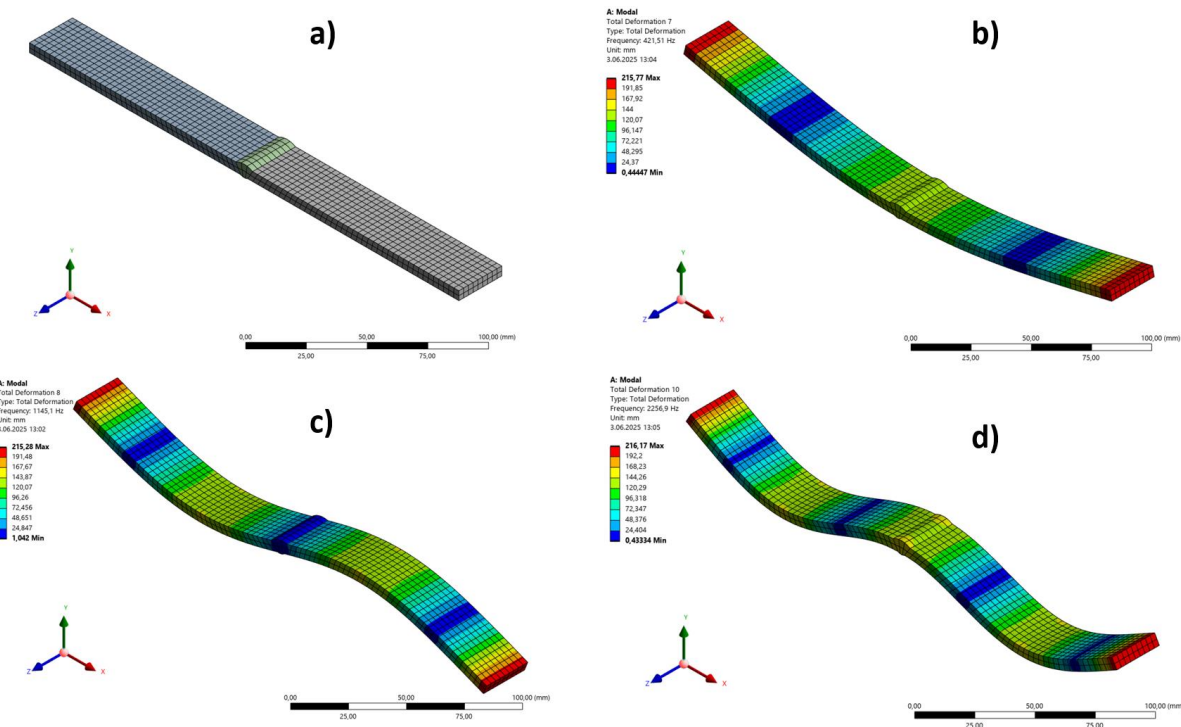


Figure 5. Isometric shapes of the welded beam, a) mesh structure, b) first mode shape, c) second mode shape, d) third mode shape.

The results of the numerical modal analysis of the reference specimen and the welded specimens with different welding root widths are shown in Table 5. The percentage difference values presented in Table 5 were calculated according to equation 4. The geometrical variation in the top and bottom of the beam in the center of the beam due to welding has a significant effect on the vibration characteristics of the beam. According to the Euler-Bernoulli equation in Eq.1, the two main parameters affecting the natural frequency are the effect of mass and volume (ρAl^4) and the effect of structural stiffness (EI).

$$\text{Percentage Difference} = \frac{\text{Reference specimen} - \text{Welded specimen}}{\text{Reference specimen}} \cdot 100 \quad (4)$$

Table 5. Numerical modal analysis results and percentage difference values of the reference specimen and welded specimens with different weld root widths

Natural frequencies	Reference specimen	Welding root widths					Percentage difference				
		0 mm	1 mm	2 mm	3 mm	4 mm	0 mm	1 mm	2 mm	3 mm	4 mm
1 st Frequency (Hz)	415.95	414.33	418.74	419.59	420.45	421.51	-0.4	0.7	0.9	1.1	1.3
2 nd Frequency (Hz)	1145.1	1145.1	1145.1	1145.1	1145.1	1145.1	0.0	0.0	0.0	0.0	0.0
3 rd Frequency (Hz)	2240.3	2230.8	2248.7	2251.3	2253.8	2256.9	-0.4	0.4	-0.5	0.6	0.7

Compared to the reference specimens, both mass and volume and structural stiffness values increased with the increase in volume in the weld zone.

- In specimens with welding root widths of 0 mm. (Figure 1.b), a decrease in natural frequency values was observed (Rao, 2019; Etin-osa & Achebo, 2017). In this case, the mass and volume change played a more dominant role than the stiffness change.
- As the welding root width increased from 1 mm to 4 mm (Figure 1.c-f), there was an increasing trend in the natural frequency values. This indicates that structural stiffness takes a more dominant role with increasing weld root width. Therefore, in such specimens joined by butt welding, the welding root width has a significant effect on the stiffness and natural frequency of the structure.
- The second natural frequency values for the free-free boundary condition did not change for all cases. Geometric (volume and mass) variation in the welding region had no effect on the second natural frequency values (Rao, 2019). This is due to the fact that the geometric change, which causes the mass and volume change, is located on the node region, which is located in the middle region. In the second mode shape, the node (non-vibrating) regions on the sample are shown in blue (Figure 6).

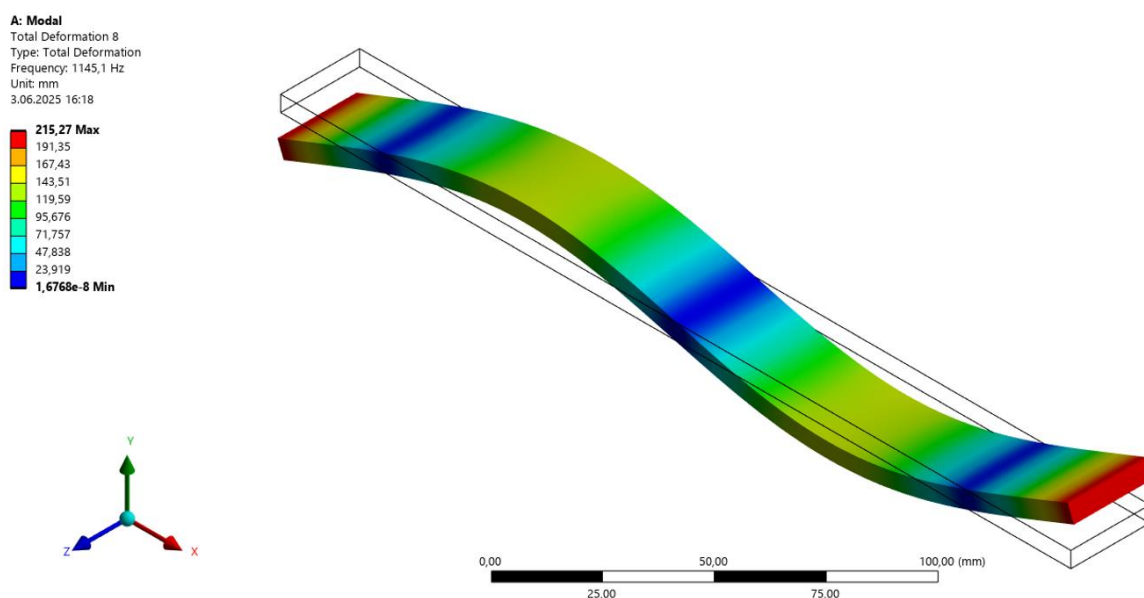


Figure 6. The node (non-vibrating) regions appearing on the specimen in the second mode (shown in blue color)

Keeping the length and width values constant, new specimens were designed to match the mass and volume values of the welded specimens. Accordingly, the thickness values were revised and new specimens were designed in the geometry of a rectangular prism and numerical modal analysis was performed. The thickness values of the specimens and the natural frequency results according to the free boundary condition are shown in Table 6. When comparing Table 5 and Table 6, the following points are worth noting. In the new rectangular prism specimens, the change in volume and mass caused a regular increase in the natural frequency values. In the welded specimens, it caused a decrease in frequency at 0 mm weld root width and an increase in frequency at larger root widths. In addition, the volume and mass changes at the node region did not cause any change in the corresponding frequency values.

Table 6. Thickness and first three natural frequencies of the reference specimen and newly designed specimens

	Reference specimen	Welding root widths				
		0 mm	1 mm	2 mm	3 mm	4 mm
Revised thicknesses (mm)	5.000	5.012	5.017	5.023	5.030	5.040
1 st Frequency (Hz)	415.95	416.95	417.36	417.86	418.47	419.28
2 nd Frequency (Hz)	1145.1	1147.8	1148.9	1150.3	1152	1154.2
3 rd Frequency (Hz)	2240.3	2245.5	2247.7	2250.4	2253.6	2257.9

4. Conclusions

In this study, numerical modal analyses were performed on aluminum alloy specimens with different root widths. The total length and width of the V-shaped specimens with butt welds were kept constant, while the welding root widths were varying from 0 mm to 4 mm in 1 mm increments. Natural frequencies and mode shapes were determined in numerical analyses performed using ANSYS Workbench® finite element software. Additionally, before analyzing the welding specimen, the natural frequency values obtained for the unwelded reference specimen using ANSYS® and Euler-Bernoulli beam theory were compared, and good agreement was observed.

According to the found results, the geometric variations in the welding region directly affected the structure's volume-mass and structural stiffness properties, and consequently its vibration characteristics. A decrease in natural frequency values was observed in the specimens with a 0 mm welding root width. The primary reason for this is that the increase in volume and mass in the welding region is more dominant than the increase in rigidity (Rao, 2019; Etin-osa & Achebo, 2017). On the other hand, as the welding root width increased from 1 mm to 4 mm, the increase in structural stiffness exhibited a more dominant characteristic than the mass-volume effect, causing an increase in natural frequency values. This situation demonstrated a direct correlation between welding geometry and the vibrational behaviour of welded structures.

The reason why the second natural frequency value remained constant in all analyses is that the welded region corresponds to the node region according to the relevant mode shape. The frequency value did not change because this region is located on the middle of the three vibration-free regions formed in the second mode shape.

In consequence, the welding region, its shape, and root width directly affect the structural rigidity and natural frequencies of the structure. This effect depends on the balance between the mass-volume variation and the increase in rigidity resulting from the welding process. With appropriate welding design, the negative effects of these geometric variations on vibration can be minimized. Welding applications performed with consideration of the location of the node areas are important in reducing the damage that large-amplitude vibrations caused by external influences can cause in the structure.

In the future, numerical and experimental optimization studies are planned to enhance the dynamic performance of welded structures using different materials and different welding root widths.

Author contribution

The entire process of the article was carried out by the corresponding author.

Declaration of ethical code

The author declares that this study does not require ethical committee approval or any legal permission.

Conflicts of interest

The author declares no competing interests.

References

AbuShanab, W. S., & Moustafa, E. B. (2018). Detection of friction stir welding defects of AA1060 aluminum alloy using specific damping capacity. *Materials*, 11(12), 2437. <https://doi.org/10.3390/ma11122437>

ANSYS Inc. (2025). *ANSYS Academic Research Mechanical, release 18.1: Coupled field analysis guide*. ANSYS Inc.

Bhusnar, M., & Sarawade, S. S. (2016). Modal analysis of rectangular plate with lap joints to find natural frequencies and mode shapes. *IOSR Journal of Mechanical and Civil Engineering*, 13(1), 6–14. <https://www.iosrjournals.org/iosr-jmce/papers/Conf15008/Vol-4/06-14.pdf>.

Chandravanshi, M., & Mukhopadhyay, A. (2013). Modal analysis of structural vibration. In *Proceedings of the ASME 2013 International Mechanical Engineering Congress and Exposition* (Vol. 14: Vibration, Acoustics and Wave Propagation, V014T15A052, pp. 1–9). American Society of Mechanical Engineers (ASME). <https://doi.org/10.1115/IMECE2013-62533>

Das, D., Pratihar, D. K., & Roy, G. G. (2020). Establishing a correlation between residual stress and natural frequency of vibration for electron beam butt weld of AISI 304 stainless steel. *Arabian Journal for Science and Engineering*, 45, 5769–5781. <https://doi.org/10.1007/s13369-020-04560-0>

de Arruda, M. V., Correa, E. O., & de Macanhan, V. B. (2023). Optimization of FEM models for welding residual stress analysis using the modal method. *Welding in the World*, 67, 2361–2372. <https://doi.org/10.1007/s40194-023-01570-y>

de Paula Macanhan, V. B., Correa, E. O., de Lima, A. M., & da Silva, J. T. (2019). Vibration response analysis on stainless steel thin plate weldments. *The International Journal of Advanced Manufacturing Technology*, 102(5–8), 1779–1786. <https://doi.org/10.1007/s00170-019-03297-x>

Etin-osa, C. E., & Achebo, J. I. (2017). Analysis of optimum butt welded joint for mild steel components using FEM (ANSYS). *Advances in Applied Sciences*, 2(6), 100–109. <https://doi.org/10.11648/j.aas.20170206.12>

Gharehbaghi, H., Hosseini, S., & Hosseini, R. (2023). Investigation of the effect of welding residual stress on natural frequencies: Experimental and numerical study. *Iranian Journal of Science and Technology, Transactions of Mechanical Engineering*, 47, 1777–1785. <https://doi.org/10.1007/s40997-022-00588-9>

Hatifi, M. M., Firdaus, M. H., & Razlan, A. Y. (2022). Modal analysis of dissimilar plate metal joining with different thicknesses using MIG welding. *International Journal of Automotive and Mechanical Engineering*, 9, 1723–1733. <https://doi.org/10.15282/ijame.9.2013.21.0143>

Hicks, J. (2000). *Welded design: Theory and practice* (1st ed.). Woodhead Publishing.

Imran, M., & Verma, R. G. (2021). Fatigue analysis of welded joint using ANSYS: A review study. *International Journal of Scientific Research & Engineering Trends*, 7(6), 3234–3242. https://ijsret.com/wp-content/uploads/2021/11/IJSRET_V7_issue6_720.pdf

Khurshid, M. (2017). *Static and fatigue analyses of welded steel structures – Some aspects towards lightweight design* [Doctoral dissertation, KTH Royal Institute of Technology]. KTH DiVA. <https://www.diva-portal.org/smash/get/diva2:1070954/FULLTEXT01.pdf>

Mathers, G. (2002). *The welding of aluminium and its alloys* (1st ed.). Woodhead Publishing.

Pavani, P., Sivasankar, M. P., Lokanadham, M. P., & Mhahesh, M. P. (2015). Finite element analysis of residual stress in butt welding of two similar plates. *International Research Journal of Engineering and Technology (IRJET)*, 2(7), 479–486.

Rao, P. S., & Ratnam, Ch. (2012). Experimental and analytical modal analysis of welded structure used for vibration based damage identification. *Global Journal of Researches in Engineering (A)*, 12(1), 45–50.

Rao, S. S. (2010). *Mechanical vibrations* (5th ed.). Pearson.

Rao, S. S. (2019). *Vibration of continuous systems*. John Wiley & Sons.

Resan, S. F., & Jasim, N. A. (2022). Experimental and numerical investigation of aluminum beams: Flexural behavior section shape effect. *Misan Journal of Engineering Sciences*, 1(2), 37–49. <https://doi.org/10.61263/MJES.V1I2.19>

Thirugnanam, A., Kumar, M., & Rakesh, L. (2014). Analysis of stress in welded joint in bending and in torsion using ANSYS. *Middle-East Journal of Scientific Research*, 20(5), 580–585. <https://doi.org/10.5829/idosi.mejsr.2014.20.05.11338>